ACES Asian Chemical Editorial Society

doi.org/10.1002/asia.202400381

CHEMISTRY AN ASIAN JOURNAL Research Article

www.chemasianj.org

Self-Assembly of four Ni_{16} Molecular Wheels with Capsule and Tubular Supramolecular Architectures

Tyson N. Dais,*[a] Sören Schlittenhardt,[b] Mario Ruben,[b, c, d] Christopher E. Anson,[e] Annie K. Powell,[b, d, e] and Paul G. Plieger*[a]

Four new Ni_{16} molecular wheels with the general formula $[L_4Ni_{16}(RCOO)_{16}(H_2O)_x(MeOH)_{12-x}]$ (where H_4L = 1,4-bis((*E*)-((2′-hydroxybenzyl)imino)methyl)-2,3-naphthalenediol, and R=H or Me) have been isolated and structurally characterised. Complexes **C1**–**C3** (R=Me) were formed using nickel (II) acetate and presented as polymorphs with the same formulation of charged components. The same wheel-like architecture was observed in **C4** (R=H), which was prepared using nickel (II) formate, demonstrating the potential for further versatility of the system. In contrast to similar four-fold symmetric Ni(II) wheel clusters, measurements of the static magnetic properties of **C1** indicated the presence of dominant antiferromagnetic interactions and an $S = 0$ ground state.

Introduction

The chemistry of discrete polynuclear coordination clusters and the resulting properties from their varied geometries, has flourished over the past few decades. Supramolecular assemblies are found in all areas of chemistry, from catalysis and drug transport to optoelectronics and single molecule magnets.[1–9] The field of molecular magnetism seeks to exploit the single magnetic domain nature of certain compounds to explore their potential as superparamagnets. For first row transition metal clusters this arises from a combination of a large ground-state spins (*S*) and a negative zero-field splitting parameter (*D*), which leads to a non-negligible energy barrier for the reversal of magnetization. A mixed valent dodecanuclear manganese cluster, now known as Mn_{12}, was the first reported SMM in 1993 by Sessoli et al.[10] 13 years after the synthesis and structure was first reported by Lis et al.[11] The now archetypal Mn_{12} cluster exhibited the retention of magnetization in zero applied field below 4 K, and was found to have a ground-state spin of $S = 10$.

While the range of reported topologies varies greatly, some of the more common architectures include cubanes, polycubanes, paddlewheels, 1D chains, and extended 2D or 3D grids or networks. However, polynuclear metal complexes which form large wheel, ring, or bowl-like clusters have attracted considerable attention, particularly among crystallographers, due to their high symmetry and often aesthetically pleasing crystal packing. An early example of a large magnetically active molecular wheel was identified by X-ray crystallography to be a 4.2 nm wide 6-fold symmetric Mn^{II}_{84} ring, which packed as nanotubular stacks in a hexagonal close-packed arrangement, with a ground-state spin of $S = 6$.[12] An even larger ring cluster was reported by Zheng et al. in 2017, featuring 140 Gd^{III} centres within a 10-fold symmetric 6.0 nm wide ring.[13] Tsami et al. recently reported a ferromagnetically coupled hexadecanuclear Co^{II} wheel (**Co16**), self-assembled from a mixture of salicylaldehyde and $Co(OAc)_2 \cdot 4H_2O$.[14] The crystal structure of **Co16** revealed that two discrete complexes come together and interdigitate forming a dimeric cavitand, which in turn stacks into tubular arrays – a feature most commonly observed in calixarenes and related analogues.[15–17] Many other aluminium,[18–20] palladium,[21–23] and molybdenum[24–27] molecular wheels are reported throughout the literature, finding uses in molecular magnetism, catalysis, and molecular sensing or host-guest chemistry.

We herein report the synthesis and structures of the Schiff base compound 1,4-bis((*E*)-((2′-hydroxybenzyl)imino)methyl)-2,3-naphthalenediol (H_4L) and four continuously M–O–M bridged hexadecanuclear nickel (II) complexes with the general formula $[L_4Ni_{16}(RCOO)_{16}(H_2O)_x(MeOH)_{12-x}]$ (Figure 1) where R=Me for **C1** ($x = 4$), **C2** ($x = 3.5$), and **C3** ($x = 2$), and R=H for **C4** ($x = 12$). Complexes **C1**–**C3** are effectively isostructural and simultaneously crystallised from a single sample as crystal polymorphs,

[a] *Dr. T. N. Dais, P. G. Plieger*
School of Natural Sciences, Massey University, Private Bag 11 222, Palmerston North, New Zealand,
E-mail: t.dais@massey.ac.nz
p.g.plieger@massey.ac.nz

[b] *S. Schlittenhardt, M. Ruben, A. K. Powell*
Institute of Nanotechnology (INT), Karlsruhe Institute of Technology (KIT), 76344 Eggenstein-Leopoldshafen, Germany

[c] *M. Ruben*
Institut de Science et d'Ingénierie Supramoléculaires (ISIS, UMR 7006), CNRS-Université de Strasbourg, 8 Allée Gaspard Monge, BP 70028, 67083 Strasbourg Cedex, France

[d] *M. Ruben, A. K. Powell*
Institute for Quantum Materials and Technologies (IQMT), Karlsruhe Institute of Technology (KIT), 76131 Karlsruhe, Germany

[e] *C. E. Anson, A. K. Powell*
Institute of Inorganic Chemistry, Karlsruhe Institute of Technology (KIT), 76131 Karlsruhe, Germany

Supporting information for this article is available on the WWW under https://doi.org/10.1002/asia.202400381

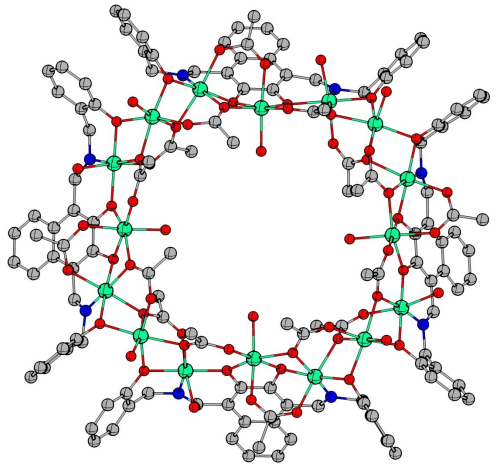

Figure 1. Generalised structure of the Ni_{16} complexes, shown with R=Me and $x=12$. C = grey, N = blue, O = red, Ni = green. H atoms are omitted for clarity.

while **C4** represents a formate analogue isolated from its own reaction mixture.

Results and Discussion

1,4-Bis((*E*)-((2′-hydroxybenzyl)imino)methyl)-2,3-naphthalenediol (H_4**L**) was prepared by the Schiff base condensation of 1,4-bisformyl-2,3-naphthalenediol[28–29] with 2-aminomethylphenol[30] in dry methanol. The ligand formed bright red block crystals upon cooling a concentrated solution of H_4**L** in MeOH or $CHCl_3$. The crystal structure was determined by XRD and was solved in the triclinic space group $P\bar{1}$. The asymmetric unit contained one molecule of H_4**L** and two molecules of the crystallisation solvent. Bond length analysis indicated that in the crystalline form the molecule exists in the keto-enamine form (C_{naphth}–O = 1.273 (2)), rather than enol-imine form (C_{naphth}–O = 1.367 (8), based on **C1**) which is observed in solution state NMR (see ESI) or upon binding to metals. Selected structural parameters are listed in Table 1. Complete synthetic details for H_4**L** and complexes **C1**–**C4** can be found in the ESI.

Complexes **C1**–**C4** were prepared by reacting four equivalents of the appropriate Ni^{II} salt in water with one equivalent of H_4**L** in MeOH at elevated temperatures for various lengths of time. Crystalline solids were obtained by the slow diffusion of

Table 1. Selected structural parameters for **C1**–**C2**.

Distance		*min/Å*	*max/Å*	*average/Å*
Ni–O_{Phen}	**C1**	1.957(4)	2.098(4)	2.006(4)
	C2	1.969(4)	2.077(4)	2.014(4)
	C3	1.960(6)	2.103(6)	2.013(6)
	C4	1.991(6)	2.108(5)	2.030(6)
Ni–OAc_{syn}	**C1**	1.928(4)	2.114(4)	2.053(4)
	C2	1.957(5)	2.124(4)	2.058(5)
	C3	1.952(7)	2.120(7)	2.056(7)
	C4[a]	1.900(9)	2.131(8)	2.045(8)
Ni–OAc_{anti}	**C1**	2.170(4)	2.178(4)	2.174(4)
	C2	2.089(4)	2.213(4)	2.137(4)
	C3	2.049(5)	2.189(6)	2.130(6)
	C4	2.069(6)	2.085(8)	2.078(6)
Ni – $O_{H_2O/MeOH}$	**C1**	2.016(5)	2.175(5)	2.096(5)
	C2	2.053(5)	2.172(5)	2.100(5)
	C3	1.996(8)	2.194(8)	2.078(8)
	C4	2.014(8)	2.138(4)	2.061(8)
Angle		*min/°*	*max/°*	*average/°*
Ni–O_{Phen}–Ni	**C1**	99.8(2)	119.4(2)	106.5(2)
	C2	97.4(2)	116.8(2)	104.2(2)
	C3	97.7(2)	117.1(3)	104.2(3)
	C4	95.7(3)	117.2(2)	103.0(3)
Ni–O_{OAc}–Ni[b]	**C1**	93.9(2)	94.8(2)	94.4(2)
	C2	92.1(1)	96.4(2)	93.7(2)
	C3	90.7(3)	96.9(3)	93.8(3)
	C4[a]	91.8(4)	96.3(2)	94.7(3)

[a] Distances and angles for **C4** refer to formate rather than acetate. [b] The Ni–O_{OAc}–Ni angles given are for the *anti*-bridging mode of the carboxylate groups.

diethyl ether into concentrated methanolic solutions of the complex. All four complexes have a pseudo-calixarene bowl-like geometry, with the 16 Ni^{II} ions forming a roughly isogonal octagonal narrow inner-rim and the naphthalene backbones splaying outward to form the wide outer-rim of the bowl. In all complexes, the ligand binds a Ni^{II} ion centrally between the catechol group, with a Ni^{II} ion either side within the *ONO* pockets, and shares a Ni^{II} ion bound by each of the phenol side arm of two ligand units, in an overall $5.2_{12}2_{23}2_{34}2_{45}1_21_4$ fashion, using Harris notation.[31–32] The carboxylate groups are observed to bind in both 2.11 (axial only) and 3.21 (axial and equatorial) modes, with three out of four Ni^{II} centres having three carboxylate contacts and the remaining Ni^{II} only having two.

Complex **C1** was prepared by refluxing H_4**L** with $Ni(OAc)_2 \cdot 6H_2O$ in damp methanol for at least 7 days. **C1** crystallised in the polar tetragonal space group P4nc with $Z = 2$ ($Z' = 0.25$) and $x = 4$ as large green blocks. The asymmetric unit consists of two structurally independent quarter-ring fragments, $[LNi_4(Oac)_4(H_2O)(MeOH)_2]$, each of which generate a full unit complex by 4-fold rotation. The two distinct Ni_{16} units generated by symmetry from the asymmetric unit display different handedness, which are best differentiated by the position of the axially coordinated water molecules. Figure 2 (a) and (b) shows each fragment from the asymmetric unit; where the water cap of fragment (a) is coordinated to the centrally bound Ni^{II} centre and will be endo to the bowl, while the water cap of fragment (b) is coordinated to one of the Ni^{II} centres bound within the ONO pocket and will be exo to the bowl. Through crystal packing, two Ni_{16} units of **C1** with opposite handedness come together in the form of a molecular capsule (Figures 3 and S2). The dimeric Ni_{16} capsule found in **C1** nestle together facilitated by a nearly 30° rotation along the 4-fold rotation axis, and has a total height slightly over 3 Å less than the sum of the heights of each **C1** fragment (see z values in Table 2), demonstrating the large degree of overlap or interdigitation in the capsule complex similar to what was observed in the Co_{16} complex of Tsami et al.[14]

Complex **C2** was obtained in conjunction with **C1** as bright green plates which crystallised in the monoclinic space group

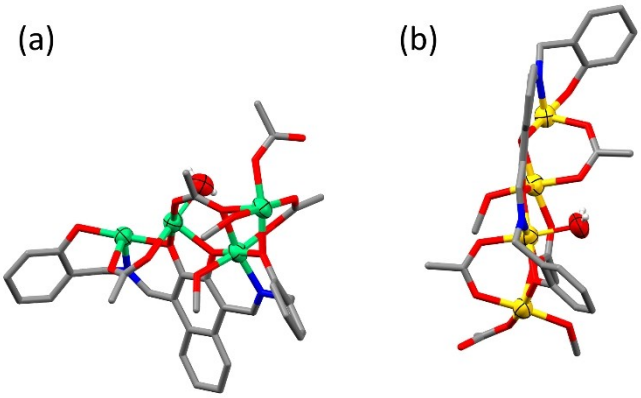

Figure 2. X-ray crystal structure showing both Ni_4 fragments from the asymmetric unit of **C1**, with non-water hydrogen atoms omitted for clarity. Thermal ellipsoids of metal and O_{H_2O} atoms are shown at 50%. C = grey, N = blue, O = red, Ni = green/orange.

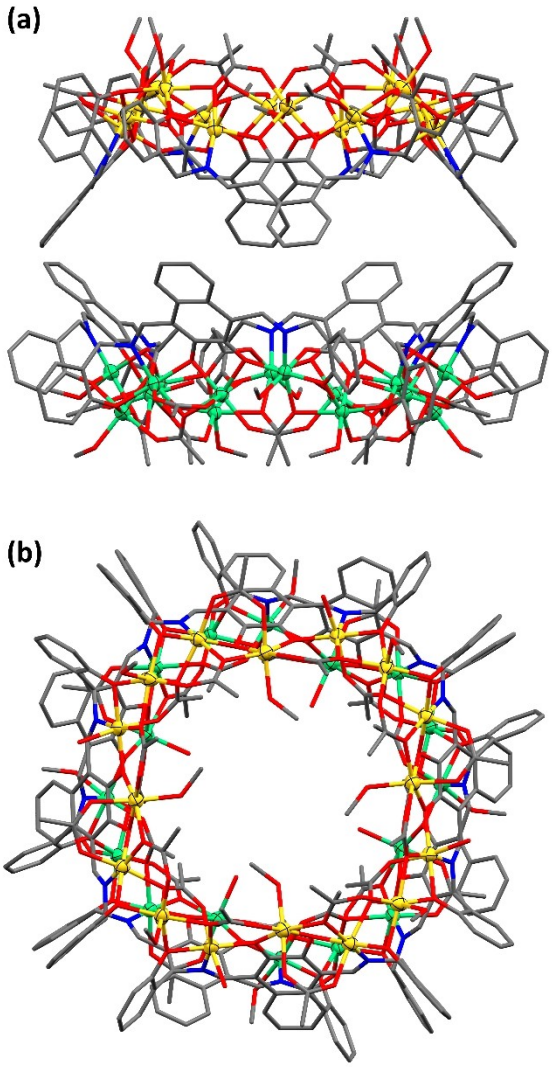

Figure 3. X-ray crystal structure of **C1** showing two Ni_{16} units packed together as a molecular capsule, viewed along the crystallographic *a*-axis (a) and *c*-axis (b), with hydrogen atoms omitted for clarity. Thermal ellipsoids of metal atoms are shown at 50%. C = grey, N = blue, O = red, Ni = green/orange.

Table 2. Cross-sectional dimensions of Ni_{16} units within each complex.

Complex	*x*/Å	*y*/Å	*z*/Å
C1[a]	25.89	25.89	12.88
C1[b]	24.84	24.84	14.02
C1^{capsule}	27.04	27.04	23.74
C2[a]	24.51	24.95	13.93
C2[b]	25.94	25.52	13.92
C3	25.64	24.84	13.92
C4	27.37	24.96	13.60

$P2_1/n$ with $Z = 8$ ($Z' = 2$) and $x = 3.5$. The two Ni_{16} units within the asymmetric unit of **C2** have the same handedness and connectivity pattern but differ by the presence of three axially

coordinated water molecules in one complex vs four in the other. The crystal packing of this complex (Figures S6 and S7) results in open bowls for the same formulation in *x* coming together narrow-rim-to-narrow-rim in the form of an elliptic hyperboloid. Pale green needles of **C3** were also observed to form from the same solution, which crystallised in the monoclinic space group *C2/c* with $Z=8$ ($Z'=1$) and $x=2$. The asymmetric unit contains a full Ni_{16} complex with both water molecules *endo* to the bowl and packs in a staggered arrangement with no further large-scale architectures observed. This form of the acetate based Ni_{16} complex was the least commonly obtained. Complexes **C2** and **C3** could be produced in larger amounts, relative to **C1**, when the reaction was run for three to five days. Optimised conditions for the crystallisation of a single polymorph have yet to be found. Isolation of pure samples of **C2** and **C3** by crystal picking was found to be unsuccessful due to the samples rapid loss of crystallinity upon the evaporation of diethyl ether.

To both better identify a preferred packing geometry and influence the M–O–M bridging angles for potential magneto-structural correlations, the preparation of Ni_{16} complexes featuring different carboxylic acid analogues (formate, trifluoroacetate, glycinate, glycolate, and benzoate) was attempted. Of these, only the formate-based analogue, **C4**, produced sufficient materials for structural characterisation. Complex **C4** was prepared in the same manner as **C1** with $Ni(HCOO)_2\cdot 2H_2O$ in place of $Ni(OAc)_2\cdot 6H_2O$, and crystallised as small green blocks in the enantiomorphic trigonal space group $P3_121$ with $Z=3$ ($Z'=0.5$) and $x=12$. The molecular cross-section dimensions of **C4** exhibit a significant asymmetry, with side lengths of ca. 2.5 and 2.7 nm, much larger than any asymmetry observed in complexes **C1**–**C3** (see Table 2). The crystal packing of **C4** forms tubular voids along all three crystallographic axes, through each complex along the crystallographic *a*- and *b*-axes (Figures S13 and S14, respectively) and formed by three complexes via a three-fold rotation axis parallel to the crystallographic *c*-axis (Figure S15). Due to the relatively large unit cell dimensions and presence of large void spaces **C1**–**C4** were treated with solvent masks to account for the diffuse electron density. The solvent accessible voids in **C1**–**C4** were calculated to occupy between 15.7% and 24.2% of the unit cell volumes, further details can be found in the ESI.

The static magnetic properties of the Ni_{16} ring in **C1** were investigated. The room temperature value of the $\chi_M T$ product, 16.95 $cm^3 K mol^{-1}$, is close to the theoretical value for 16 uncoupled Ni^{II} spins with $g=2.05$ (16.81 $cm^3 K mol^{-1}$), although for Ni^{II} in an octahedral coordination environment a significant zero-field splitting parameter, *D*, is likely. On cooling, $\chi_M T$ remains at this value until about 60 K, below which temperature it decreases to reach 9.47 $cm^3 K mol^{-1}$ at 2 K (Figure 4). A logarithmic plot (Figure S16) suggests $\chi_M T$ extrapolates to zero at $T=0$ K. The magnetization curves measured at 2, 3, 4, and 5 K (Figure 4 inset) are all rather similar, showing no indication of saturation and with that at 2 K reaching only 4.52 μ_B at 7 T, consistent with antiferromagnetic interactions. Additionally, the non-superposition of the plotted reduced magnetisation data for **C1** (Figure S17) indicates the presence of significant

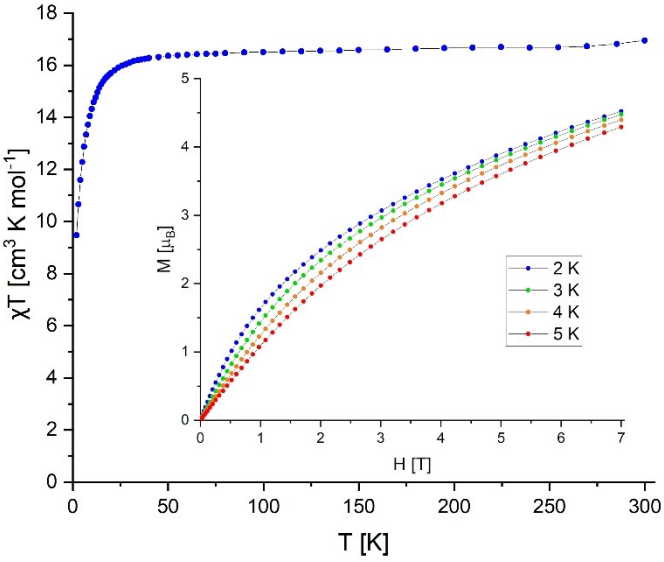

Figure 4. Plot of the $\chi_M T$ product vs *T* for **C1**, measured under an applied field of 0.1 T, with variable temperature magnetisation plots for **C1** inset.

anisotropy in the system and/or the presence of low-lying magnetic states.

A quantitative analysis of the magnetic properties of **C1** is beyond the scope of this paper, however it is clear that antiferromagnetic interactions are dominant within the ring, in agreement with the Curie-Weiss plot (Figure S18), which gives $\theta=-2.0$ K. The data thus indicate that **C1** has a spin ground state with $S=0$, which is probably not well separated from the excited states. This is in contrast to previously reported Ni_{12}[33] and Ni_{20}[34] rings; the former exhibits ferromagnetic interactions with an $S=12$ ground state, while in the latter both ferromagnetic and antiferromagnetic interactions are present, also resulting in a ground state with $S=12$.

The 4-fold molecular symmetry of the ring implies that it is made up of four equivalent Ni_4 units, with a repeating pattern of four *J* values around the ring. The mean Ni–O–Ni angles between pairs of Ni^{II} centres within the Ni_4 unit are 98.0, 95.7, 98.6 and 116.0°, suggesting a J_1–J_2–J_1*–J_3 repeating pattern Figure 5. Previous magneto-structural reports of polynuclear Ni^{II} complexes have highlighted the influence of the Ni–O–Ni bridging angle on the sign and relative magnitude of magnetic exchange couplings, with larger bridging angles (exceeding ca. 98°) resulting in larger antiferromagnetic contributions.[35–40] A counter-complementary effect of bridging carboxylate groups paired with bridging phenolato groups has also been reported.[36,41]

In order to better identify the sign and relative magnitudes of nearest neighbour and next-nearest neighbour magnetic exchange interactions, we performed broken symmetry DFT calculations on a model of **C1** (Figure S19). In line with previous reports, the calculations indicated J_1, J_1*, and J_3 correspond to moderate to weak antiferromagnetic couplings (−9.76, −2.51, and −0.84 cm^{-1}, respectively), while J_2 is weakly ferromagnetic with a calculated value of +5.00 cm^{-1}. The difference between

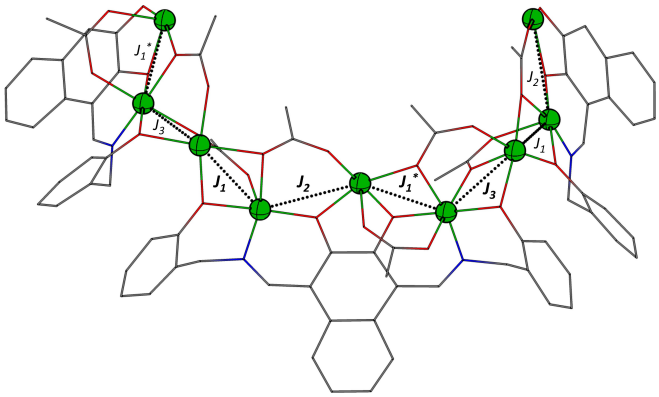

Figure 5. Substructure of **C1** labelling the four unique nearest-neighbour magnetic interactions. Hydrogen atoms, water, and methanol molecules have been omitted for clarity. C = grey, N = blue, O = red, Ni = green.

J_1 and J_1* values is attributed to the presence of non-planar phenolato bridging groups vs the relatively planar catecholate bridge. The d-orbitals in the former has weak overlap with the phenolato p_z(O) and moderate overlap with the p_x(O) orbitals (with Mulliken spin populations of 0.026 and 0.058, respectively) whereas the latter allows for a greater average overlap with the catecholate p_x(O) and p_y(O) orbitals (with Mulliken spin populations of 0.042 and 0.045, respectively). Spin-densities and unrestricted corresponding orbitals for each calculation have been visualized in Figures S20–S28. There are two unique next-nearest neighbour interactions facilitated by *syn,anti*–O–C–O-(carboxylate) bridges; J_4' which occurs eight times around the Ni16 ring, and J_5' which only occurs unidirectionally four times around the ring, i.e. within the asymmetric unit Ni2 A and Ni4 A are not bridged, however Ni2 A is bridged to the nearest symmetry generated Ni4 A. Both of these next-nearest neighbour interactions are weakly ferromagnetic with averages values of 0.04 cm^{-1} (J_4') and 0.53 cm^{-1} (J_5').

The ground state of the Ni_{16} ring will have $S = 0$, regardless of the sign of J_2. Even if this coupling is ferromagnetic giving four pairs of adjacent Ni^{II} centres with parallel spin within the ring, the three antiferromagnetic couplings between such pairs will result in two of the pairs of Ni^{II} having their spins both "up", and the other two their spins both "down". This is in contrast to the previously mentioned Ni_{20} rings, which also have fourfold symmetry.[34] Here, the extra Ni^{II} in each repeating unit means that any ferromagnetic couplings within the ring will now result in four pairs of Ni^{II} around the ring with their spins all parallel, and a ferrimagnetic ground state with $S = 12$ was in fact observed for their Ni_{20} ring.

Conclusions

A symmetric Schiff base ligand and four related hexadecanuclear Ni^{II} complexes have been prepared and structurally characterised. Complexes **C1**–**C4** all self-assemble in the form of L_4Ni_{16} supramolecular wheels, ligated by H_4**L** and carboxylic acid groups. Complexes **C1**–**C3** were isolated from the same reaction mixture utilising $Ni(OAc)_2 \cdot 4H_2O$ as the nickel source. While control over the formation of specific polymorphs has not yet been obtained, it was found that longer reaction times led to increased amounts of **C1** upon crystallisation, conversely, shorter reaction times led to a qualitative increase in the presence of **C2** and **C3**. These three complexes are nearly isostructural and present unique crystal morphologies corresponding to their symmetry. Complex **C4** was obtained as green blocks, similar to **C1**, by the 1:4 reaction of H_4**L** with $Ni(HCOO)_2 \cdot 2H_2O$, however its unexpected crystallisation into the trigonal space group $P3_121$ meant the Ni_{16} units of **C4** did not pack into dimeric capsules, as in **C1**. Static magnetic susceptibility and magnetisation measurement for a polycrystalline sample of **C1**, gave a $\chi_M T$ product of 16.95 $cm^3 K mol^{-1}$ at 300 K which only decreased to 9.47 $cm^3 K mol^{-1}$ at 2 K, and an unambiguously unsaturated magnetization at 7 T and 2 K of 4.52 μ_B. These measurements are consistent with theoretical calculations also indicate dominant antiferromagnetic interactions, and the presence of significant anisotropy. While the Hilbert space required to accurately and quantitatively model these Ni_{16} complexes is prohibitively large, it is clear that antiferromagnetic interactions dominate the magnetic properties of **C1**. Based on the similarities of the bond lengths and angles given in Table 1, antiferromagnetic interactions are also likely to dominate the magnetic properties of polymers **C2** and **C3**, as well as analogue **C4**.

Author Contributions

TND: conceptualisation, investigation, data curation, formal analysis, visualisation, writing – original draft, writing – review & editing. SS: investigation, data curation, formal analysis. MR: supervision. CEA: investigation, data curation, formal analysis, visualisation, writing – review & editing. AKP: supervision. PGP: supervision, project administration, writing – review & editing.

Notes and references

The authors have cited the following additional references in the ESI.[42–58] Deposition Numbers 2164495–2164499 contain the supplementary crystallographic data for this paper. These data are provided free of charge by the joint Cambridge Crystallographic Data Centre and Fachinformationszentrum Karlsruhe Access Structures service.

Acknowledgements

TND and PGP thank Massey University for the ward of Massey University Doctoral Scholarship for Māori to TND. AKP, MR, and SS thank the Helmholtz Foundation POF MSE for financial support. The authors wish to acknowledge the use of New Zealand eScience Infrastructure (NeSI) high-performance computing facilities as a part of this research. New Zealand's national facilities are provided by NeSI and funded jointly by

NeSI's collaborator institutions and through the Ministry of Business, Innovation and Employment's Research Infrastructure programme. Open Access publishing facilitated by Massey University, as part of the Wiley - Massey University agreement via the Council of Australian University Librarians.

Conflict of Interests

The authors declare no conflict of interest.

Data Availability Statement

The data that support the findings of this study are available in the supplementary material of this article.

Keywords: Metallacycles · Schiff base ligands · Self-assembly · Supramolecular architectures · Transition metals

[1] D. M. Kaphan, M. D. Levin, R. G. Bergman, K. N. Raymond, F. D. Toste, *Science* **2015**, *350*, 1235–1238.
[2] Z. J. Wang, K. N. Clary, R. G. Bergman, K. N. Raymond, F. D. Toste, *Nat. Chem.* **2013**, *5*, 100–103.
[3] Z. Feng, T. Zhang, H. Wang, B. Xu, *Chem. Soc. Rev.* **2017**, *46*, 6470–6479.
[4] J.-M. Lehn, *Science* **1993**, *260*, 1762–1763.
[5] K. Kalyanasundaram, M. Grätzel, *Coord. Chem. Rev.* **1998**, *177*, 347–414.
[6] L. F. Lindoy, K.-M. Park, S. S. Lee, *Chem. Soc. Rev.* **2013**, *42*, 1713–1727.
[7] O. Roubeau, R. Clérac, *Eur. J. Inorg. Chem.* **2008**, *2008*, 4325–4342.
[8] D. Maniaki, E. Pilichos, S. P. Perlepes, *Front. Chem.* **2018**, 461.
[9] T. Glaser, *Chem. Commun.* **2011**, *47*, 116–130.
[10] R. Sessoli, D. Gatteschi, A. Caneschi, M. Novak, *Nature* **1993**, *365*, 141–143.
[11] T. Lis, *Acta Crystallogr. Sect. B* **1980**, *36*, 2042–2046.
[12] A. J. Tasiopoulos, A. Vinslava, W. Wernsdorfer, K. A. Abboud, G. Christou, *Angew. Chem. Int. Ed.* **2004**, *43*, 2117–2121.
[13] X.-Y. Zheng, Y.-H. Jiang, G.-L. Zhuang, D.-P. Liu, H.-G. Liao, X.-J. Kong, L.-S. Long, L.-S. Zheng, *J. Am. Chem. Soc.* **2017**, *139*, 18178–18181.
[14] P. A. Tsami, T. G. Tziotzi, A. B. Canaj, M. K. Singh, S. J. Dalgarno, E. K. Brechin, C. J. Milios, *Dalton Trans.* **2022**, *51*, 15128–15132.
[15] Y.-J. Zhu, Y. Gao, M.-M. Tang, J. Rebek, Y. Yu, *Chem. Commun.* **2021**, *57*, 1543–1549.
[16] J.-F. Wang, L.-Y. Huang, J.-H. Bu, S.-Y. Li, S. Qin, Y.-W. Xu, J.-M. Liu, C.-Y. Su, *RSC Adv.* **2018**, *8*, 22530–22535.
[17] K. Moon, A. E. Kaifer, *J. Am. Chem. Soc.* **2004**, *126*, 15016–15017.
[18] L. Geng, C.-H. Liu, S.-T. Wang, W.-H. Fang, J. Zhang, *Angew. Chem. Int. Ed.* **2020**, *59*, 16735–16740.
[19] S. Yao, W.-H. Fang, Y. Sun, S.-T. Wang, J. Zhang, *J. Am. Chem. Soc.* **2021**, *143*, 2325–2330.
[20] Y. Zhang, Q.-H. Li, W.-H. Fang, J. Zhang, *Inorg. Chem. Front.* **2022**, *9*, 592–598.
[21] F. Xu, H. N. Miras, R. A. Scullion, D.-L. Long, J. Thiel, L. Cronin, *PNAS* **2012**, *109*, 11609–11612.
[22] R. A. Scullion, A. J. Surman, F. Xu, J. S. Mathieson, D. L. Long, F. Haso, T. Liu, L. Cronin, *Angew. Chem. Int. Ed.* **2014**, *53*, 10032–10037.
[23] L. G. Christie, A. J. Surman, R. A. Scullion, F. Xu, D.-L. Long, L. Cronin, *Angew. Chem. Int. Ed.* **2016**, *55*, 12741–12745.
[24] A. Müller, E. Krickemeyer, J. Meyer, H. Bögge, F. Peters, W. Plass, E. Diemann, S. Dillinger, F. Nonnenbruch, M. Randerath, *Angew. Chem. Int. Ed.* **1995**, *34*, 2122–2124.
[25] T. Liu, E. Diemann, H. Li, A. W. Dress, A. Müller, *Nature* **2003**, *426*, 59–62.
[26] D. Zhong, F. L. Sousa, A. Müller, L. Chi, H. Fuchs, *Angew. Chem. Int. Ed.* **2011**, *50*, 6931–6931.
[27] A. Müller, E. Krickemeyer, H. Bögge, M. Schmidtmann, C. Beugholt, P. Kögerler, C. Lu, *Angew. Chem. Int. Ed.* **1998**, *37*, 1220–1223.
[28] S. H. M. Mehr, H. Depmeier, K. Fukuyama, M. Maghami, M. J. MacLachlan, *Org. Biomol. Chem.* **2017**, *15*, 581–583.
[29] T. N. Dais, R. Takano, T. Ishida, P. Plieger, *Dalton Trans.* **2022**, *51*, 1446–1453.
[30] Y. Herzig, L. Lerman, W. Goldenberg, D. Lerner, H. E. Gottlieb, A. Nudelman, *J. Org. Chem.* **2006**, *71*, 4130–4140.
[31] S. G. Harris, Crystallographic and modelling studies of organic ligands on metal surfaces, *Ph.D Thesis*, The University of Edinburgh, **1999**.
[32] R. A. Coxall, S. G. Harris, D. K. Henderson, S. Parsons, P. A. Tasker, R. E. Winpenny, *J. Chem. Soc. Dalton Trans.* **2000**, 2349–2356.
[33] H. Andres, R. Basler, A. J. Blake, C. Cadiou, G. Chaboussant, C. M. Grant, H. U. Güdel, M. Murrie, S. Parsons, C. Paulsen, *Chem. Eur. J.* **2002**, *8*, 4867–4876.
[34] K. I. Alexopoulou, A. Terzis, C. P. Raptopoulou, V. Psycharis, A. Escuer, S. P. Perlepes, *Inorg. Chem.* **2015**, *54*, 5615–5617.
[35] A. D. Katsenis, V. G. Kessler, G. S. Papaefstathiou, *Dalton Trans.* **2011**, *40*, 4590–4598.
[36] S. S. Woodhouse, T. N. Dais, E. H. Payne, M. K. Singh, E. K. Brechin, P. G. Plieger, *Dalton Trans.* **2021**, *50*, 5318–5326.
[37] M. K. Singh, G. Rajaraman, *Inorg. Chem.* **2019**, *58*, 3175–3188.
[38] M. A. Halcrow, J.-S. Sun, J. C. Huffman, G. Christou, *Inorg. Chem.* **1995**, *34*, 4167–4177.
[39] K. K. Nanda, L. K. Thompson, J. N. Bridson, K. Nag, *J. Chem. Soc. Chem. Commun.* **1994**, 1337–1338.
[40] L. Ballester, E. Coronado, A. Gutierrez, A. Monge, M. F. Perpinan, E. Pinilla, T. Rico, *Inorg. Chem.* **1992**, *31*, 2053–2056.
[41] S. Hazra, S. Bhattacharya, M. K. Singh, L. Carrella, E. Rentschler, T. Weyhermueller, G. Rajaraman, S. Mohanta, *Inorg. Chem.* **2013**, *52*, 12881–12892.
[42] APEX4, SADABS, and SAINT, Bruker AXS Inc. Madison, WI, USA **2016**.
[43] G. Sheldrick, *Acta Crystallogr. Sect. A* **2015**, *71*, 3–8.
[44] G. Sheldrick, *Acta Crystallogr. Sect. C* **2015**, *71*, 3–8.
[45] O. V. Dolomanov, L. J. Bourhis, R. J. Gildea, J. A. K. Howard, H. Puschmann, *J. Appl. Crystallogr.* **2009**, *42*, 339–341.
[46] F. Neese, *Wiley Interdiscip. Rev.: Comput. Mol. Sci.* **2012**, *2*, 73–78.
[47] A. Becke, *Phys. Rev. A: At. Mol. Opt. Phys.* **1988**, *38*, 3098.
[48] K. Yamaguchi, Y. Takahara, T. Fueno, *Applied Quantum Chemistry* Springer, **1986**, 155–184.
[49] T. Soda, Y. Kitagawa, T. Onishi, Y. Takano, Y. Shigeta, H. Nagao, Y. Yoshioka, K. Yamaguchi, *Chem. Phys. Lett.* **2000**, *319*, 223–230.
[50] C. Lee, W. Yang, R. G. Parr, *Phys. Rev. B* **1988**, *37*, 785.
[51] S. Grimme, J. Antony, S. Ehrlich, H. Krieg, *J. Chem. Phys.* **2010**, *132*, 154104.
[52] S. Grimme, S. Ehrlich, L. Goerigk, *J. Comput. Chem.* **2011**, *32*, 1456–1465.
[53] J. K. Buchanan, T. N. Dais, P. G. Plieger, *Phys. Chem. Chem. Phys.* **2022**, *24*, 4407–4414.
[54] S. S. Woodhouse, T. N. Dais, A. Etcheverry-Berríos, E. K. Brechin, J. R. Lane, P. G. Plieger, *Inorg. Chem.* **2022**, *61*, 17819–17827.
[55] A. Schäfer, H. Horn, R. Ahlrichs, *J. Chem. Phys.* **1992**, *97*, 2571–2577.
[56] F. Weigend, *Phys. Chem. Chem. Phys.* **2006**, *8*, 1057–1065.
[57] F. Weigend, R. Ahlrichs, *Phys. Chem. Chem. Phys.* **2005**, *7*, 3297–3305.
[58] F. J. Arnáiz, *J. Chem. Educ.* **1995**, *72*, A200.

Manuscript received: April 4, 2024
Revised manuscript received: June 20, 2024
Accepted manuscript online: June 24, 2024
Version of record online: ■■, ■■

RESEARCH ARTICLE

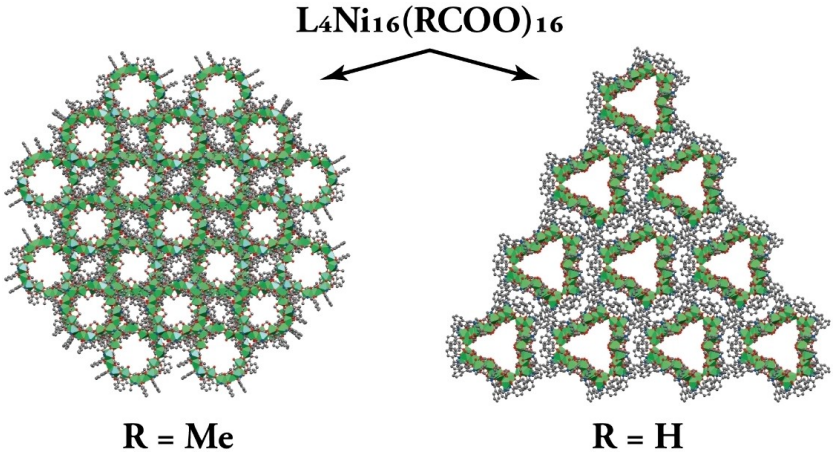

Four hexadecanuclear nickel-based molecular wheels generated from carboxylate salts show vastly different crystal packing, including the formation of a molecular capsule.

Magnetic measurements of the acetate derivative indicate an $S=0$ ground state, unusual for nickel metallacycles.

Dr. T. N. Dais, S. Schlittenhardt, M. Ruben, C. E. Anson, A. K. Powell, P. G. Plieger**